SPATIAL METHODS FOR CHARACTERISING CARBON ANODES FOR ALUMINIUM PRODUCTION

Camilla Sommerseth[1], Rebecca Jayne Thorne[1], Stein Rørvik[2], Espen Sandnes[3], Arne Petter Ratvik[2], Lorentz Petter Lossius[3], Hogne Linga[3] and Ann Mari Svensson[1]

[1]Dept. of Materials Science and Engineering, Norwegian University of Science and Technology, NO-7491 Trondheim, Norway
[2]SINTEF Materials and Chemistry, NO-7465 Trondheim, Norway
[3]Hydro Aluminium AS, Årdal, Norway

Keywords: Carbon Anodes, Anisotropic Sponge Coke, Isotropic Coke, Carbon Consumption

Abstract

Pilot test anodes were designed by Hydro Aluminium for laboratory studies using controlled blends of <2 mm aggregate from two single source cokes. Spatial and imaging methods were used to characterise anode surfaces with respect to consumption, density, pore distribution and real active area before and after electrolysis. The methods include X-ray computed tomography (CT), confocal microscopy, scanning electron microscopy (SEM) and energy-dispersive X-ray spectroscopy (EDS). It was found that during electrolysis, the electrolyte does not completely wet the carbon inside large pores on the surface. Hence, even large pores do not contribute to the electrochemically active surface area. Large grains of isotropic cokes and anisotropic sponge cokes are consumed at approximately the same rate and bubble coke in anisotropic sponge cokes are consumed at a slower rate than the bulk material. This is due to higher resistivity through the bubble coke.

Introduction

Producing stable and good quality anodes is critical for satisfactory performance of anodes during electrolysis. The industry is facing deteriorating coke quality, and previously rejected fuel grade coke of isotropic character now has to be accepted as anode grade coke [1, 2]. These changes in coke quality will affect impurity levels, impurity elements and mixing and baking processes [3, 4]. Physical parameters like density, specific electric resistivity, air permeability, mechanical strength, coefficient of thermal expansion, thermal shock resistance, thermal conductivity, CO_2 and air reactivity and dusting are commonly used in the aluminium industry to characterise carbon anodes to evaluate their quality. These tests are done on non-electrolysed anodes before they have been used in cells, but there is not necessarily a good correlation between these properties and the anode performance during electrolysis. The present work is part of a greater research program called Hal Ultra Performance (HAL UP) where the aim is to predict the quality of anodes electrochemically with better testing before and after electrolysis.

When dealing with anodes and electrolysis to produce aluminium, one important factor is how the electrolyte wets the anodes. Wettability is an important factor for gas bubble growth, formation and release. Different coke types may affect wetting properties of anodes towards the electrolyte. Wetting tests have traditionally been done using the sessile drop method, where electrolyte is placed on an unpolarised anode surface, heated and the wetting angle measured when the electrolyte has melted. This gives an idea of the wetting conditions; although wetting conditions are thought to change during polarisation of the carbon surface. Poor wetting between electrolyte and anode is often said to cause the anode effect [5, 6], although this has been disputed by other researchers [7]. When performing the sessile drop method it has been found that the lower the alumina concentration, the poorer wetting [7].

Through powerful spatial imaging methods the understanding on how anodes are consumed during electrolysis can be improved. Wetting properties of the electrolyte toward the anode surface and pores in the anode structure can be investigated by CT scanning. Adams et al. [8] showed how CT scanning can be used to view interior of anode materials. Picard et al. [3, 9, 10] have shown the use of CT scanning to determine apparent density and detect cracks in anodes. The method is non-destructive and enables reconstruction of the internal morphology of the core samples,

thus providing useful information about both pristine and electrolysed anodes. Confocal microscopy can be used to investigate the roughness of anodes before and after electrolysis, and increases the understanding of how anodes are consumed during electrolysis. The opportunity to create large area maps in SEM and create EDS elemental maps of larger areas of anode surfaces also gives important information on the distribution of various impurity elements and coke grains, and how they might affect anode consumption locally.

In this work, wetting of the carbon anode during electrolysis, as well as possible preferential consumption of coke grains (anisotropic grains with and without high content of sulphur, bubble coke, and isotropic grains) has been investigated by CT scanning, SEM/EDS and confocal microscopy in order to better understand anode performance during electrolysis. Cracks in anodes formed during the baking process is also investigated by CT scanning.

Experimental

Pilot anodes were specially designed and made at Hydro Årdalstangen for these experiments. They were produced from industrial grade coke and pitch. The anodes were made of <2 mm coke aggregate from two different single source cokes and produced to a common sieving curve from ball mill product (fines ¡63 μm), 0-1 and 1-2 mm fractions. This was done to ensure a comparatively smooth and representative exposed surface area.

Three different anode materials were studied:

- Anode A = made from 100% single source anisotropic sponge coke A (fines from sponge coke)

- Anode B = made from 100% single source isotropic coke B (fines from isotropic coke)

- Anode C = 49% isotropic coke B, 51% anisotropic sponge coke A (fines from sponge coke)

The anodes were characterized by complementary image analysis techniques to investigate the pore distribution on the surface and interior in the anodes and electrolyte penetration into pores before and after electrolysis by using CT and investigating the pore structure in anodes before electrolysis by confocal

microscopy. SEM/EDS were used to perform element mapping on large surface areas.

For the CT mapping an anode assembly similar to the one shown in Figure 1 in Thorne et al. [4] was used ($\emptyset$ = 10 mm, height of anode sample = 5 mm). The anode test piece was covered with a BN piece on the top and bottom to create a horizontal anode surface area. A graphite rod in the middle served as electrical contact. The anodes were scanned both before and after electrolysis of 1.0 A/cm^2 for 1800 s in a cryolitic melt of cryolite ratio of 2.3, saturated in alumina. The anodes were withdrawn from the electrolyte with current still on (hot-pulled). CT was performed on a Nikon XT H225 ST machine. A molybdenum reflection target was used. Settings for the imaging were: voltage of 110 kV, current of 200 μA, integration time of 1 second, 1440 projections per revolution, distance from source to sample was 35.1 mm, distance from source to detector was 1124.8 mm and the voxel size (combination of "volume" and "pixel" to denote the resolution) was 6.2 μm. Three different software from Nikon Metrology were used to create the CT images: Inspect-X (used to control the x-ray generator, sample table and collecting images), CT Pro 3D (used to edit parameter files for reconstruction of CT images) and CT Agent (used for reconstruction of CT images). MÅ HØRE MED STEIN ANG ETTERANALYSE OG SOFTWARE

A different anode assembly was used for the confocal microscopy and SEM/EDS scans. The anodes were rods of $\emptyset$ = 10 mm and the surface of interest were the horizontal end pieces. These end pieces were grinded with SiC paper step-wise down to P#4000. The distribution of impurities on the anode surfaces was determined by SEM/EDS and the changes in topography of the anode surface before and after electrolysis was studied by 3D confocal microscopy. The confocal microscope was an Infinitefocus by Alicona and the system used an optical 3D surface metrology. The resolution was 410 nm. The equipment used for the SEM/EDS image mapping was a low vacuum SEM, Hitachi S-3400N and the software used was Aztec by Oxford Instruments. Large area maps using SEM/EDS were created. The entire end piece area of the anode core was investigated by creating over 400 small area maps with an overlap of 20%. These maps were then stitched together to one large map using the Aztec software. 3D maps from confocal microscopy showed the surface roughness of the grinded samples. Electrolysis was performed on the anodes at

a current density of 1.0 A/cm^2, in a melt saturated with alumina, and with a cryolite ratio of 2.3 for 1500 s. The electrolyte left on the anode test pieces after electrolysis was removed using AlCl$_3$(s). Confocal microscopy measurements were repeated for the electrolysed samples in order to investigate changes in the surface roughness.

Results and Discussion

CT Imaging

Figures 1, 3 and 2 show two cross-sections before and after electrolysis through the core of two different anode parallels of the three anode materials (A-C), obtained by the CT method. The dense core in the middle is the aforementioned graphite rod that the anode test piece is threaded around, in order to create electrical contact. The before and after images have been matched to fit the exact rotation and height in the anode piece and allows for identification of the electrolyte wetting of pores and carbon consumption on the surface. The CT images give a close to frozen view of the electrolyte-carbon surface interaction during electrolysis as the electrolyte freezes very quickly on the anode surface when it is taken out of the furnace.

In Figure 1 cross-sections of an anode (Ø = 10 mm) made of anisotropic sponge coke is shown. The single source coke used for anode A is inhomogeneous, with some small areas of bubble coke. Anode A is a well-mixed anode with few large pores. Figure 4 shows a zoom-in on an area of anode A parallel 2 with bubble coke and matrix before and after electrolysis. It is interesting to see that the bubble coke is consumed at a much lower rate than the bulk material. The bubble coke appear also to have poorer wetting towards the electrolyte, as the electrolyte layer is very thin. One explanation to why the bubble coke are consumed at a lower rate can be decreased electronic conductivity through these high porosity grains. Another explanation can be that pores are filled with CO$_2$ gas, causing an overpressure that block the electrolyte from penetrating the pores. The former explanation seems more likely.

Anode B is displayed in Figures 2 (a) and (b). This anode is made from pure isotropic coke. The anode samples are full of large pores indicating a poor recipe for anode making, with an improper ratio between fines and larger coke grains and poor baking and

mixing conditions. Even large pores are not filled with electrolyte, and the images suggest that the electrolyte forms a bridge at the neck of the pore. It is only when pores are convex (e.g. the pore of the west end of Figure 2 (b)) that the pore walls are wetted by electrolyte and contribute to the active surface area. In those cases an edge effect is seen and the surface is evened out through electrolysis.

Images of scans of anode C are shown in Figure 3 (a) and (b). Anode C is a mixture of anisotropic (51%) and isotropic coke (49%). The isotropic coke grains are easily detectable as spheres in the anisotropic matrix. The anode is more porous than Anode A and long narrow cracks can be seen in the matrix close to the isotropic coke grains. Two zoom-in pictures of anode B and C shown in Figure 5, show that these narrow cracks can only be seen in the anodes of mixtures of coke A and B, not in anode B made of pure single cokes. The cracking occurs due to different thermal expansion of the coke types during baking. In Figure 3 (a) a white inclusion (probably of silicon, calcium or iron) is seen in the non-electrolysed image in the North West corner near the anode surface. After electrolysis, this inclusion is gone, and has left a void. It is reasonable to assume that this inclusion has been dissolved into the electrolyte. The electrolyte has not penetrated well into the void, suggesting poor wetting between the electrolyte and the anode when the anode is polarised. No preferred consumption between isotropic and anisotropic cokes can be seen.
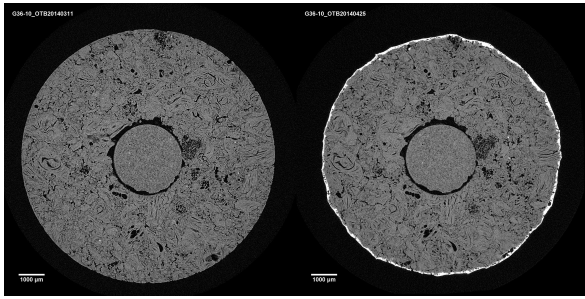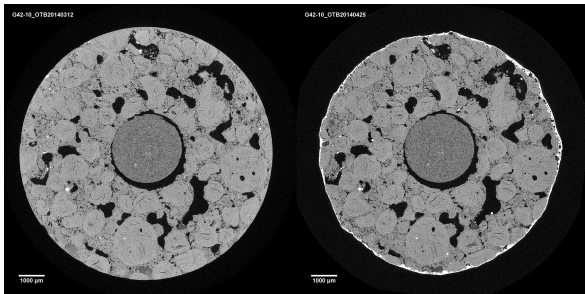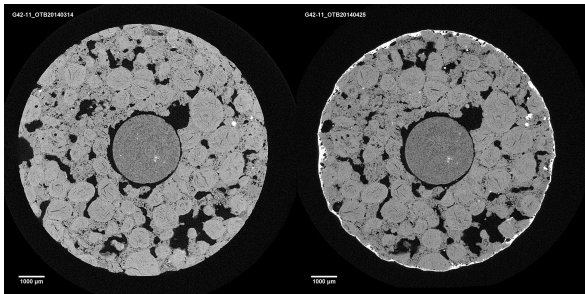
(a)
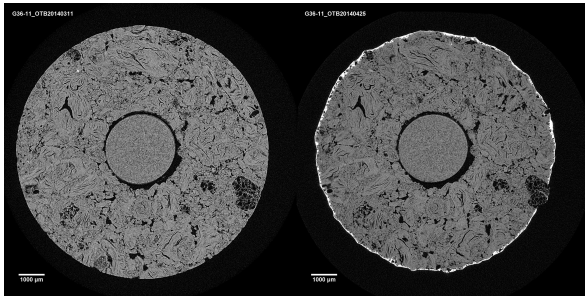
(b)

Figure 1: Anode A (a) Parallel 1. (b) Parallel 2.
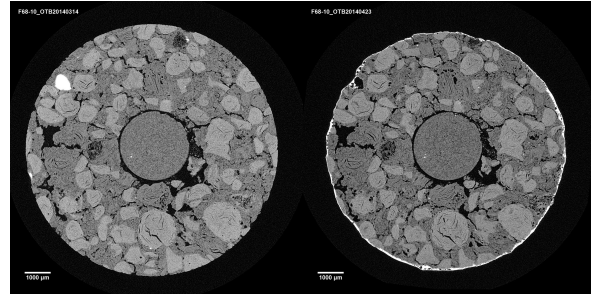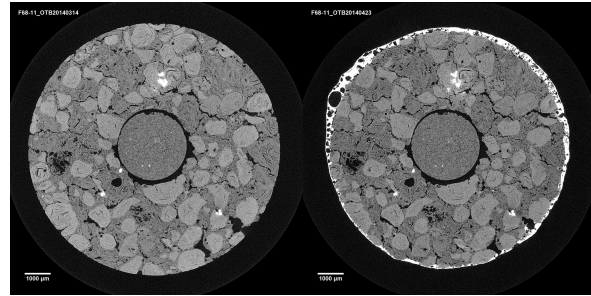

(a)

(b)

Figure 2: Anode B (a) Parallel 1. (b) Parallel 2.
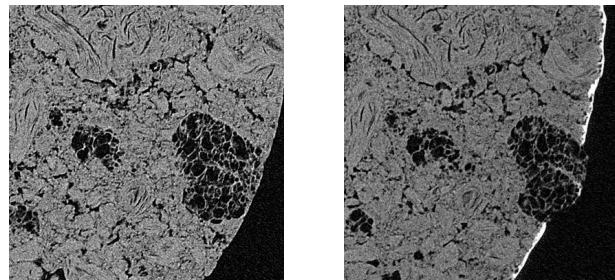

(a)

(b)

Figure 3: Anode C (a) Parallel 1. (b) Parallel 2.

(a)   (b)

Figure 4: Anode A zoom-in, parallel 2 (a) Before electrolysis. (b) After electrolysis.

Confocal microscopy images and SEM/EDS maps

Figures 6 (a)-(x) show images from SEM/EDS investigations and confocal microscopy. EDS maps for other elements than sulphur have been excluded due to space limitations, although elements like Ca, Fe, Si and Zn were spread on the surface of the anode test piece. Vanadium was not detected for anode A, but was found to "outline" the large spherical isotropic coke grains for anodes B and C.

Figures 6 (d), (h) and (t) show contour images of the surfaces of anode A (both parallels) and anode
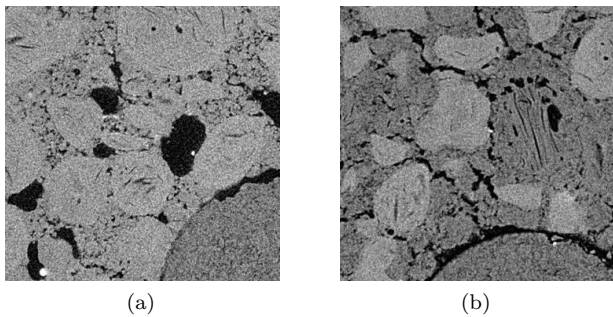
(a)   (b)

Figure 5: Zoom-in on anode cracks (a) Anode B. (b) Anode C.

C (parallel 1) after electrolysis, where the electrolyte has been removed using an $AlCl_3$ solution. On all those images it can be seen that bubble coke sticks out, suggesting low carbon consumption. The CT images support these findings. Also, there are indications that areas high in sulphur may have been consumed at a higher rate than the matrix. This can be due to different structure of the coke grain high in sulphur compared to the regular coke grains. To verify this, more experiments need to be done, and possibly other methodologies need to be used. The removal of electrolyte by $AlCl_3$ is a weak point of the methodology of confocal imaging after electrolysis. Parts of the anode can detach when performing this procedure and the electrolyte proved difficult to remove from the anode despite being submerged into the $AlCl_3$ solution for a long time. Figures 6 (l) and (p) suggest that the fines have been consumed at a higher rate than the larger isotropic coke grains. However, the CT images do not support this suggesting that removal of electrolyte on the carbon surface is a weak part of the methodology. The CT images do not support any preferred consumption between the large isotropic coke grains and the fines and pitch binder. However, the fines in anode B was of isotropic character, whereas the fines in anodes A and C where of anisotropic character. Hence, Figures 6 (t) and (x) suggest that isotropic fines detach more easily from the anode surface when removing the electrolyte. This can be due to poor wetting between coke and pitch during anode fabrication.

Conclusion

CT imaging is a powerful and non-destructive method to investigate interior and structure (carbon porosity and coke grain distribution) of carbon anodes for alu-minium production both before and after electrolysis. The method gives valuable information on cracks and porosity, and can thus indicate ways to optimise baking and mixing temperatures as well as pitch/coke interactions. CT also gives information on the consumption of the carbon surface when electrolysed. Large area mapping in SEM/EDS enables the investigation of relatively large anode surfaces in terms of elemental distribution of impurities and homogeneity. Confocal microscopy can be used to determine the real surface area including the contribution from pores on a given surface. It can also be used to investigate the anode surface after electrolysis to a certain degree. The most important findings in this work is that during electrolysis there is no preferred consumption between large grains of anisotropic and isotropic coke. For sponge cokes, bubble coke are consumed at a slower rate than the matrix and electrolyte does not penetrate even larger pores unless they are of convex character.
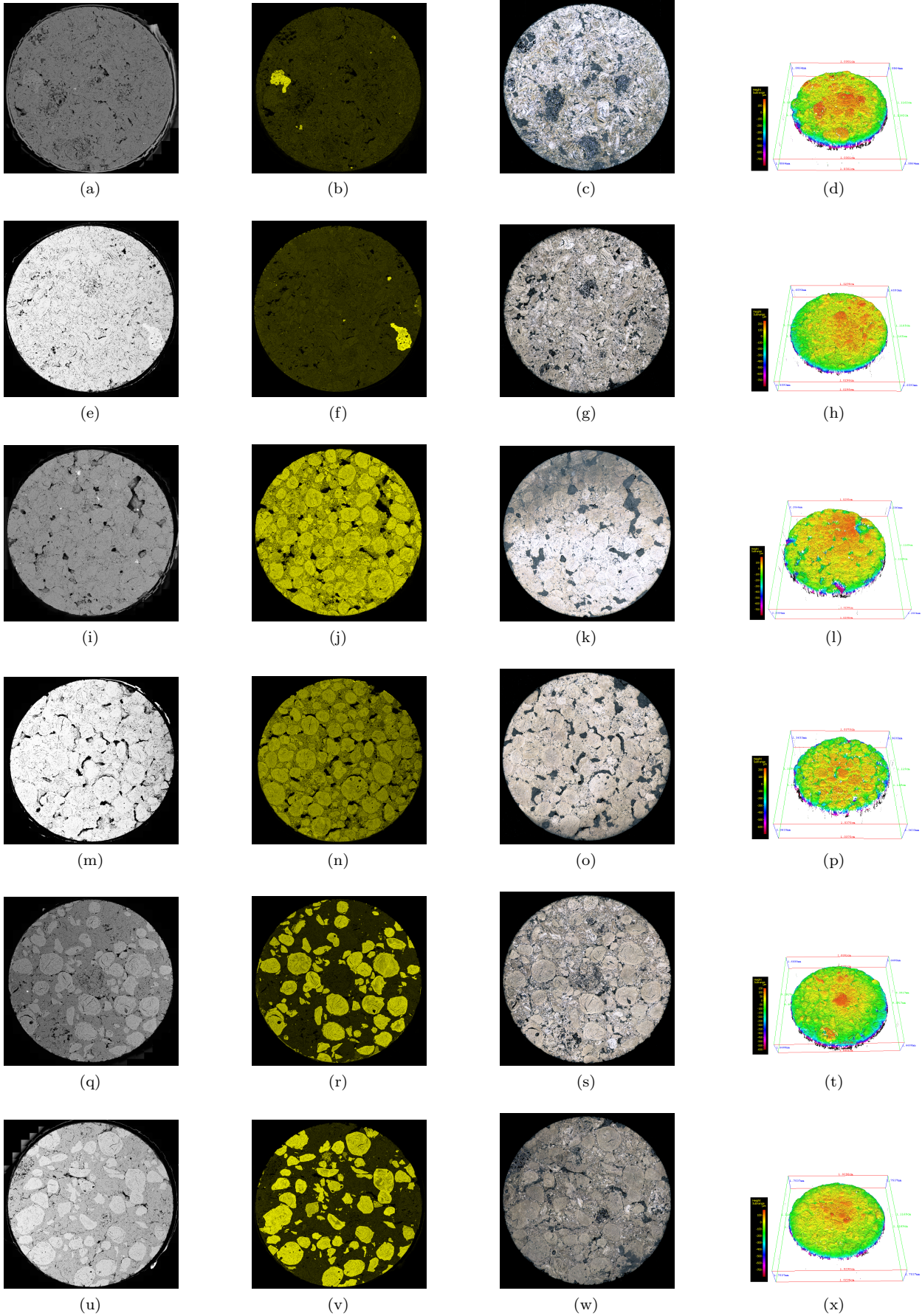
Acknowledgement

Figure 6: Anode A, parallel 1 ((a)-(d)) and parallel 2 ((e)-(h)). Anode B, parallel 1 ((i)-(l)) and parallel 2 ((m)-(p)). Anode C, parallel 1 ((q)-(t)) and parallel 2 ((u)-(x)). (a), (e), (i), (m), (q) and (u) are SEM surface maps. The pictures are stiched together of over 400 single pictures. (b), (f), (j), (n), (r) and (v)

References

[1] L. Edwards, N. Backhouse, H. Darmstadt, and M.-J. Dion. Evolution of anode grade coke. *Light metals*, pages 1207–1212, 2012.

[2] L. Edwards, F. Vogt, M. Robinette, R. Love, A. Ross, M. McClung, R.J. Roush, and W. Morgan. Use of shot coke as an anode raw material. *Light metals*, pages 985–990, 2009.

[3] D. Picard, J. Lauzon-Gauthier, C. Duchesne, H. Alamdari, M. Fafard, and D. Ziegler. Automated crack detection method applied to CT images of baked carbon anode. *Light metals*, pages 1275–1280, 2014.

[4] R.J. Thorne, C. Sommerseth, A.M. Svensson, E. Sandnes, L.P. Lossius, H. Linga, and A.P. Ratvik. Understanding anode overpotential. *Light metals*, pages 1213–1217, 2014.

[5] H. Vogt. Effect of alumina concentration on the incipience of the anode effect in aluminium electrolysis. *J Appl Electrochem*, pages 779–788, 1999.

[6] H. Vogt. The anode effect as a fluid dynamic problem. *J Appl Electrochem*, pages 137–145, 1999.

[7] P. Meunier, B. Welch, M. Skyllas-Kazacos, and V. Sahajwalla. Effect of dopants on wetting properties and electrochemical behaviour of graphite anodes in molten Al_2O_3-cryolite melts. *J. Appl. Electrochem.*, pages 837–847, 2009.

[8] A.N. Adams, O. Karacan, A. Grader, J.P. Mathews, P.M. Halleck, and H.H. Schobert. The nondestructive 3-D characterization of pre-baked carbon anodes using x-ray computerized tomography. *Light metals*, pages 535–539, 2002.

[9] D. Picard, H. Alamdari, D. Ziegler, B. Dumas, and M. Fafard. Characterization of pre-baked carbon anode samples using X-Ray computed tomography and porosity estimation. *Light metals*, pages 1283–1288, 2012.

[10] D. Picard, H. Alamdari, D. Ziegler, P. St-Arnaud, and M. Fafard. Characterization of a full-scale prebaked carbon anode using X-Ray computerized tomography. *Light metals*, pages 973–978, 2011.